Research on Engineering Structures & Materials
www.jresm.org
Research Group

Research Article

Experimental research of a structural health monitoring system concept based on fiber Bragg grating sensors on composite panels of an aircraft

Maksim Soldatkin[a], Ekaterina Prilipko[b], Kirill Ibrishev[c], Konstantin Illarionov[d]

Moscow Aviation Institute (National Research University), Moscow, Russia

Article Info

Article history:

Received 14 May 2024
Accepted 15 Aug 2024

Keywords:

Fiber Bragg grating; Health monitoring system; Composite materials; Static and dynamic tests

Abstract

In the dynamic realm of aviation, ensuring the structural integrity of aircraft stands as an imperative pillar of safety and operational efficiency. Amidst this landscape, the advent of Fiber Bragg Grating (FBG) sensing technology has propelled structural health monitoring (SHM) into a new era of precision and reliability. This paper embarks on an exploration of SHM in aviation, using the transformative capabilities of FBG sensing. The primary objective was to evaluate the sensitivity of FBG-based sensors to static and dynamic loads as well as the response to defects formed upon fracture. The study involves fifteen experiments with FBG setups on a composite panel. Using interrogators, the distortions in optical signals were obtained and recalculated to provide data on deformations. Based on the results, FBG sensing technology proved to be sensitive to the mentioned load types, outputting consistent data.

1. Introduction

The aviation industry is actively trying to reduce expenses by adopting composite materials for weight reduction and cost benefits. However, the novelty of these materials and their potential risks make designers cautious. Regular evaluations of these materials can help optimise aircraft structural design. Maintenance, Repair, and Overhaul (MRO) account for a significant portion of operational costs due to the discarding of parts, despite them being structurally sound [1]. A system for continuous structural health monitoring can help address these issues and reduce costs [2]. Various sensors are used in Structural Health Monitoring (SHM), including strain gauges and piezoelectric sensors, each with their limitations such as sensitivity to electromagnetic interference [3]-[6]. Fiber Bragg Grating (FBG) sensors, immune to such interference and capable of multiplexing, offer a significant advancement. They are lightweight, compact, and can cater to various sensing needs, making them ideal for aviation applications. [7]. FBG-based SHM systems offer high sensitivity, electromagnetic interference immunity, and real-time monitoring, making them ideal for aerospace applications. They can monitor fatigue, stress, temperature, and vibrations in aircraft components, aiding in maintenance and safety. Future research should focus on advanced sensor integration, data analysis techniques, and cost reduction to enhance their capabilities and applications. FBG sensors are widely used by European Space Agency for strain and temperature measurement of structural composites [8]. The extensive use of FBG in aviation is also acknowledged in [9], where experimental tests

*Corresponding author: soldatkinmy@mai.ru
[a]orcid.org/0009-0006-6141-5906; [b]orcid.org/0000-0001-7063-5261; [c]orcid.org/0009-0006-4345-3335; [d]orcid.org/0009-0005-4534-0089
DOI: http://dx.doi.org/10.17515/resm2024.287cs0514rs

were carried out comparing the surface attached FBG sensors with resistance strain gauges. Results clearly demonstrate the superiority of FBG sensors due to higher sensitivity and accuracy of deformations read. Using embedded FBG sensors allowed for the detection of delamination in [10] as well as vibration loads in [7]. Uniaxial tension tests were conducted in [11], the difference in FBG and Vic3D system did not exceed 6%.

This study used surface attached FBG sensors (using cyanoacrylate adhesive [12]) to explore the possibilities of detecting applied loads and compare them to Rayleigh sensors. The experiments carried out involved static, dynamic, and failure loads, comparing the results of each subsequent test [13] - [17]. The outcome is evidential of FBG sensing technology demonstrating high sensitivity, consistently producing reliable data, which is proven by a series of comparative tests with various loading conditions, including destruction of a panel, results of which clearly demonstrate the smallest changes in deformations (and specifically, residual deformations). The equipment in use (interrogator x30-700) is capable of reading wavelength signals up to 1000 Hz, which is sufficient for real-time monitoring of a structure; as well as having a tolerance of 1% (in terms of wavelengths measured in the range 1510 – 1590).

2. Methods and Materials

The research utilised optical fibers from Micron Optics with an applied Fiber Bragg Grating (FBG), which serves as the sensitive element of the sensor, as well as the SM-125 measuring device. The supplied FBGs are compatible with Micron Optics' measurement equipment and can be used in measurement tasks that require deformation measurement of small parts, embed into polymer and composite materials, including carbon fiber-reinforced plastic.

This system quickly and consistently performs peak centre wavelength measurements on a 0.25 nm FBG over a wide range of input conditions and sensor signal attenuation, without the need to manipulate gain settings or peak detection parameters. In most typical cases, the main part of the data transmitted by the receiving and recording devices consists of primary readings of measured wavelengths. An FBG-based sensor is a segment of optical fiber with a periodic refractive index gradient (Bragg grating) [18]. As a result, a portion of the radiation passing through the fiber is reflected, with the wavelength at the peak of the reflection coefficient corresponding to the grating period. Any changes to this period due to physical processes (such as deformation or temperature changes) also alter the reflection wavelength of the Bragg grating [19] – [21]. In this manner, authors of [20] have conducted numerous experiments with similarly attached FBGs (using cyanoacrylate adhesive), and an analogues interrogator (with the range of 1480-1580 nm), resulting deformations of which are in the same order of magnitude as those, presented in results and discussion section of this paper. Aforementioned researchers have come across similar difficulties related to the FBG installation process.

To obtain specific values of deformations from FBG sensors, experimental results (acquired wavelengths) must be divided by 0.78 to yield deformation in μm/m, which is considered in further work. Without this division, initial raw data from the device is the relative change in wavelength; after the division, the result is micro strain over time (με) [22].

$$\lambda_{BG} = 2\Lambda n_{eff} \tag{1}$$

$$\Lambda = \Lambda_0(1 + \varepsilon) \tag{2}$$

$$\frac{dn}{d\varepsilon} = -\frac{(n)^2}{2}\left(p_{12} - \nu(p_{11} + p_{12})\right) \tag{3}$$

$$\lambda_{BG} = \lambda_{BG}(\varepsilon) \quad (4)$$

$$\frac{1}{\lambda_{BG}}\frac{d\lambda_{BG}}{d\varepsilon} \approx 0.78 \cdot 10^{-6}\mu\varepsilon^{-1} \quad (5)$$

Where
λ_{BG} – the Bragg resonance wavelength;

Λ – Bragg grating period;

n_{eff} – the effective RI (refractive index) of the fiber core for the central wavelength;

ε – deformations;

n – index of refraction;

ν – Poisson's ratio;

p_{11}, p_{12} – elastooptic tensor components

Table 1 – Metrological and technical characteristics

No	Characteristic	Value
	Interrogator	
1	Measuring device	x30-700
2	Range of wavelength measurement, nm	1510 – 1590 Tolerance ± 20
3	Range of changes in temperature, ºC	From - 40 to + 120 ± 2,0
4	Range of deformation measurement, %	0,01 – 0,25 ± 1
5	Scanning frequency, Hz	1000
6	Number of optical channels	4
	Sensors	
7	Sensing element	FBG
8	Sensitivity, pm/μm -1	~1.2
9	Coating material	Acrylate, Polyimide
10	Coating diameter, μm	145-165
11	Length, mm	10
12	Optical fiber type	Single-mode, compliant with SMF-28
13	Number of optical endings	2
14	Cable bending diameter, mm	≥17

The research procedure using (FBG) consists of:

- Preparation of samples, tools, fixtures, and sensors;
- Assembly of the data analysis system for the deformation of the object under study;
- Selection of sensor adhesion technology, load calculations;
- Direct adhesion of sensors to the sample;
- Calibration of the monitoring system;
- Conducting experiments by applying various types of loads.

Values of metrological and technical characteristic of the measuring apparatus and optical fibers used in the research are presented in table 1.

2.1. The Research Objective and Testing Procedure

The study investigates the sensitivity of FBG-based sensors to static loads and impacts of varying energy applied to a composite panel with both honeycomb-filled and solid parts. A schematic view of the panel is presented in Fig. 1, with the thickness values (h) averaged.

The health monitoring system consists of the recording equipment - NTM130 optical interrogator; the strain sensors - a single-mode fiber with a thickness of 145 micrometres (10 micrometres for the core, 125 micrometres for the cladding, and 145 micrometres for the protective coating). The operational wavelength for this type of sensors ranges from 1.5 to 1.6 micrometres. Software – Micron Optics. Sensors are attached to the surface of the panel with dimensions of 1 m^2 using a cyanoacrylate adhesive, both on the solid part and on the area filled with honeycomb.

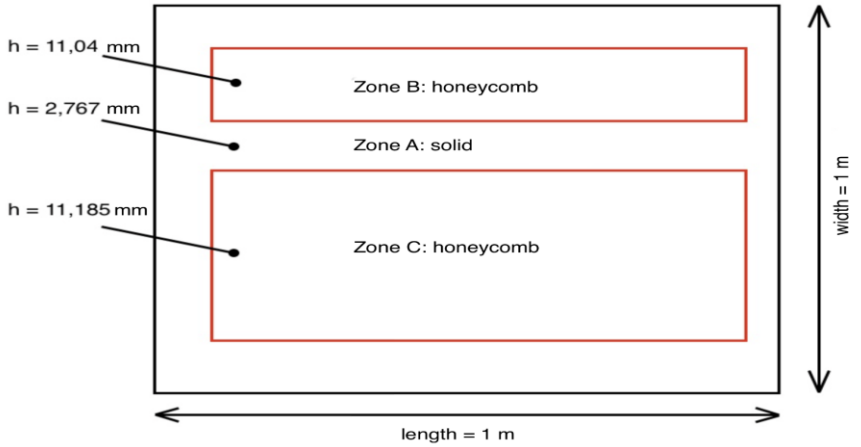

Fig. 1. Schematic view of the panel, zones of interest and geometrical parameters

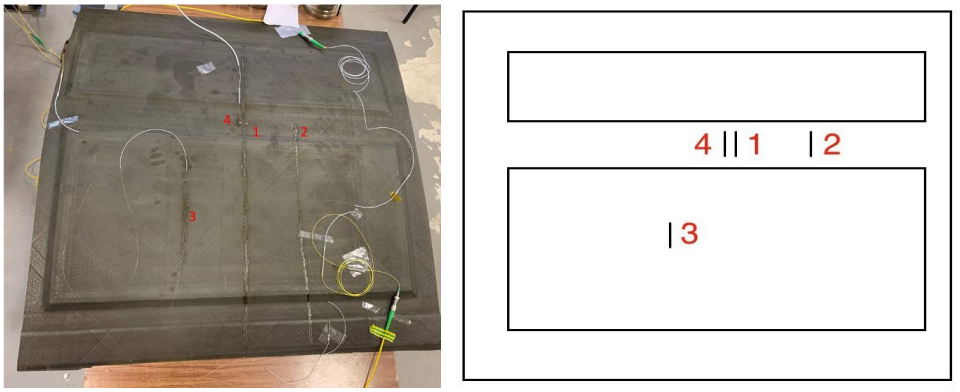

(a) (b)

Fig. 2. Composite panel with FBG installed a) General layout; b) Schematic representation of FBG-based sensors disposition

The positioning of the sensors and the general layout of the panel is presented in Fig. 2 a). The numeration corresponds to the order in which sensor were attached as well as the approximate location of FBG. The terms "acrylate" and "polyimide" sensors refer to the type of

protective coating applied to the fiber optic sensor. The types of sensors attached to the plate, which measures 1 m^2, are illustrated in Fig. 2 b) as follows:

- Acrylate sensor on the monolithic part of the plate;
- Acrylate sensor on the monolithic part of the plate (damaged grating);
- Acrylate sensor on the honeycomb part of the plate;
- Polyimide sensor on the monolithic part of the plate.

The sampling frequency in all tests (both static and dynamic loads) was 1 kHz. Static tests were conducted by loading the panels with weights of 1, 5 and 10 kg.

2.2 Description of the Conducted Tests

Experiments 1 through 4 served a purpose of calibrating the equipment and setting up the workspace. In the static tests the loading step was 1 kg at a time on each side of the sensor. Next, a reduction of 5 weights of 1 kg each took place, followed by the application of a 5 kg weight. This process was repeated with a 10 kg weight. As a result, the panel was subjected to a total load of 25 kilograms. In the subsequent static experiments, the positioning of the loads, the methodology of application, and the mass were analogous to those previously outlined. The loaded zones of the panel are represented in Fig. 3.

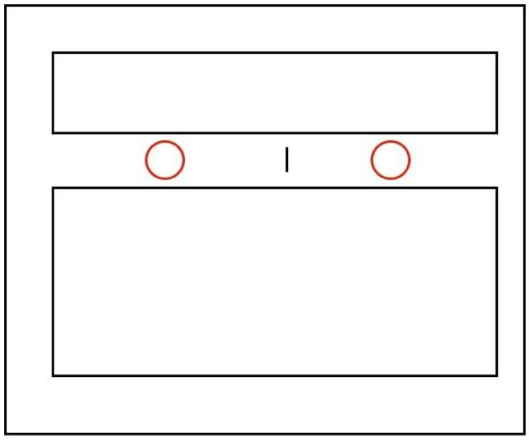

Fig. 3. The zones loading was applied

The dynamic tests consisted of applying individual impacts along different zones of the panel from various heights using a handmade drop test rig (appearance presented in Fig. 4 a). The order of impacts in experiment 2 is schematically represented in the Fig. 4 b).

In subsequent experiments, four sensors were used. Acrylic sensor No. 3 was attached to the honeycomb part of the plate (Zone C) to compare the resulting data depending on the plate structure. The difference between acrylic (1) and polyimide (4) sensors was examined to compare different types of optical fiber coating, where no significant differences were found. Acrylic sensors are more prone to damage during adhesion, whereas polyimide sensors exhibit less stiffness.

The plate was subjected to static loads, dynamic loads of varying energy, drilling, and hammering loads, list of experiments is presented in table 2. After each event that damaged the plate (12, 14), static tests were carried out. Data processing takes the changes of deformations into account.

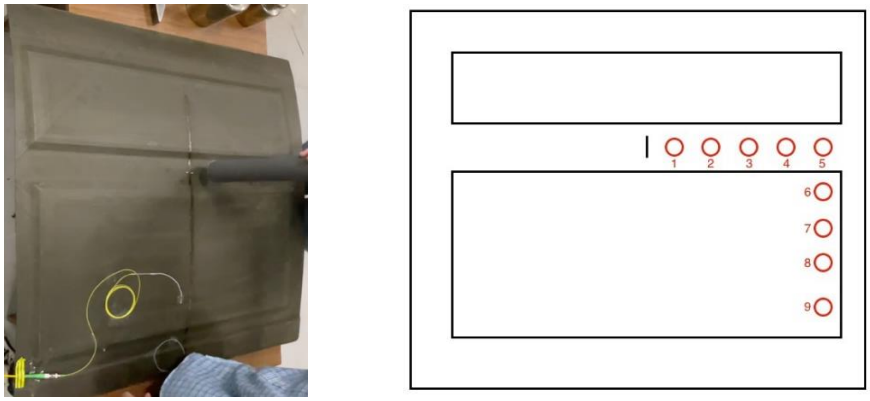

(a) (b)

Fig. 4. (a) Device for applying impact loads and (b) diagram and order of single impact with a drop test rig in experiment 2

The decoding of the graphs, loads, and sensors in the experiment results are as follows:

- Acrylic sensor on the monolithic part of the plate (red graph, labelled "central");
- Acrylic sensor on the monolithic part of the plate (pink graph, damaged sensor, labelled "side");
- Acrylic sensor on the honeycomb part of the plate (black graph, labelled "on honeycombs");
- Polyimide sensor on the monolithic part of the plate (blue graph, labelled "polyimide").

Table 2. List of experiments carried out

No exp.	Number of sensors	Sensor type	Loading type
1	1	Acrylate	Static
2	1	Acrylate	Dynamic
3	2	Acrylate	Static
4	2	Acrylate	Dynamic
5	4	3 acrylate ones, 1 polyimide one	Static
6	4	3 acrylate ones, 1 polyimide one	Static
7	4	3 acrylate ones, 1 polyimide one	Dynamic
8	4	3 acrylate ones, 1 polyimide one	Dynamic
9	4	3 acrylate ones, 1 polyimide one	Dynamic
10	4	3 acrylate ones, 1 polyimide one	Dynamic
11	4	3 acrylate ones, 1 polyimide one	Dynamic
12	4	3 acrylate ones, 1 polyimide one	Drilling
13	4	3 acrylate ones, 1 polyimide one	Static
14	4	3 acrylate ones, 1 polyimide one	Fracture using a hammer
15	4	3 acrylate ones, 1 polyimide one	Static

The investigation of static deformation during the operation of an aircraft using fiber-optic sensors is necessitated by the need for continuous real-time monitoring of the aircraft's structural integrity. Fiber-optic sensors, due to their high sensitivity and measurement accuracy, afford the opportunity for detailed analysis of deformations and stresses that occur in the aircraft's structure under various operating conditions. Conducting such investigative measurements allows for the timely detection of potential defects, cracks, or fatigue damage that may lead to emergency situations during flight. Thus, the use of fiber-optic sensors for monitoring static deformation during aircraft operation is a necessary step to ensure flight safety and extend the aircraft's service life.

The use of fiber-optic sensors to measure impact energy during an aircraft's operation is critical for analysing dynamic loads that result from external influences on the aircraft's structure. Fiber-optic sensors are valued for their high sensitivity and ability to measure a wide range of parameters, which enables a precise calculation of impact energy and evaluation of its effect on the aircraft's structural integrity. These measurements facilitate the identification of potential weak points in the structure that are vulnerable to damage from significant impacts, thereby enhancing flight safety and the overall reliability of air transportation.

3. Results and Discussions

The resulting deformations of the first static experiment (gradual loading of the panel) are shown in Fig. 5. Here, the small loading steps can be clearly seen in the graph 5 a), represent each consecutive installation of a 1 kg weight, while bigger steps demonstrate their removal (5 to 10 kg at a time).

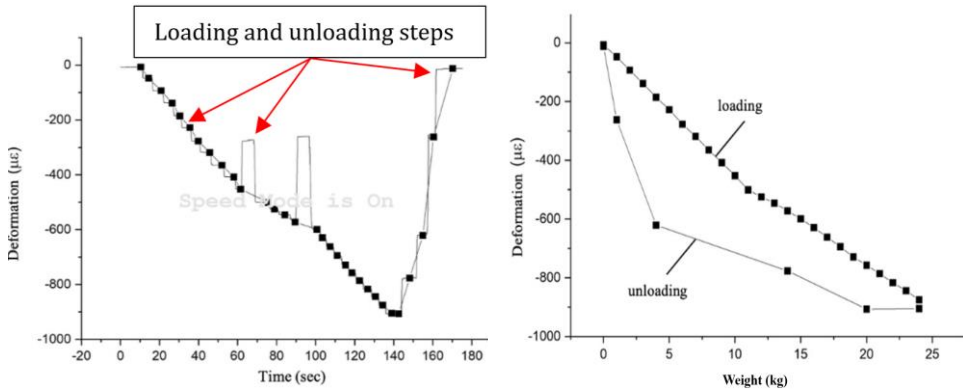

(a) (b)

Fig. 5. A deformation-time graph (a) and deformation-load graph (b) resulting from the first static test measured by an acrylic sensor

Fig. 6 presents the deformation-time graph based on the conducted dynamic test 2 in which the loads were applied using a handmade drop test rig (appearance presented in Fig. 4 a). On this graph, the moment of each impact is clearly visible, demonstrating the sharp sensitivity of the FBG-based sensors to dynamic loads. After each subsequent strike there is a noticeable amount of noise, representing the removal of the rig. The initial deformation in this and subsequent experiments is non-zero because of the residual deformations from the static experiments.

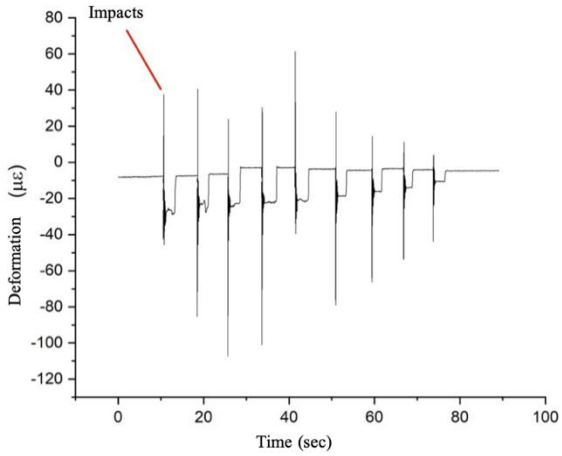

Fig. 6. Deformation-time graph resulting from dynamic tests measured by an acrylic sensor

Experiment 7 involved impacts from a consistent height of 1 meter across the entire length, at various distances from the sensors, of the monolithic part of the composite plate. The place and order of impacts using the drop rig is schematically represented in the Fig. Fig. 7 (a), and the deformation-time graphs are presented in the Fig. Fig. 7 (b) and Fig. Fig. 8. All the sensors had a clear and similar response. A clear tendency to the increased magnitude of deformations is seen upon impacts 2 and 3 as those are positioned the closest to the FBG sensors which is evident of higher sensitivity within the short range of a sensor. This dependency would be useful in an FBG-array for determining an exact position of an impact.

The residual deformations resulting from the impact should be taken upon consideration while analyzing the results as to not be confused with the impact itself. Experiment 14 involved the fracture of the panel at two locations (both monolithic and honeycomb-filled parts of the composite panel) using hammer impact as to see how FBG sensors would react to the destruction of a said composite material. The locations of impacts and subsequent defects are shown in Fig. 9. The external appearance of the destroyed panel is shown in Fig. 10.

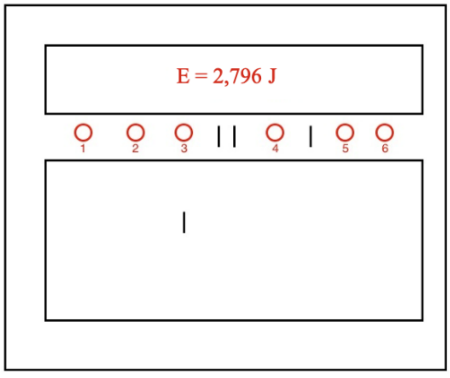

(a)

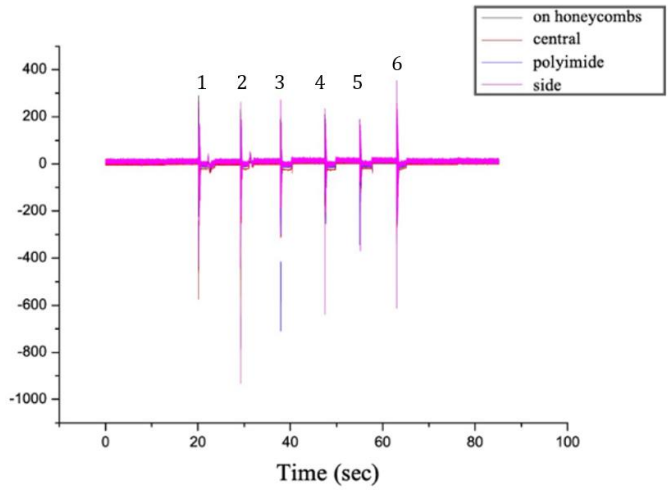

(b)

Fig. 7. (a) Order and disposition of dynamic impacts and (b) the deformation-time graph resulting from dynamic tests measured by three acrylic sensors and one polyimide sensor

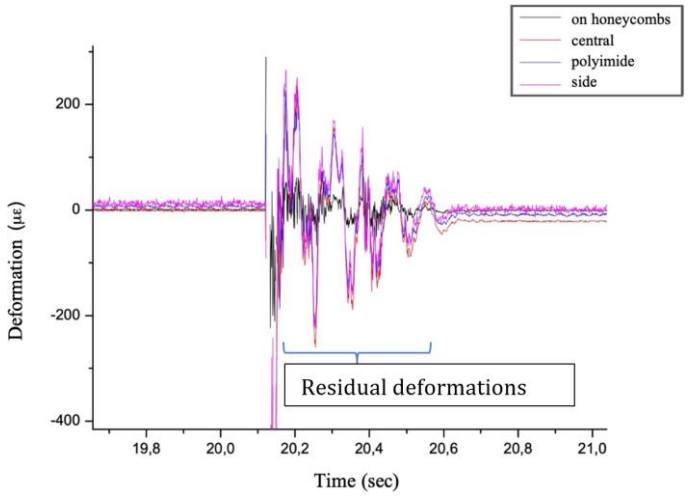

Fig. 8. The deformation-time graph of the first impact close up

These strikes were carried out for further comparison of the static experiments before and after destruction of the composite of the panel with respect to the remaining stresses and deformations introduced to the structure.

Fig. 11 – 12 present the results of static tests of all sensors post-impact, post-drilling, and after fracture with a hammer. It can be observed that the sensor located on the honeycomb part experiences the least deformation in each experiment, while the side-located acrylic sensor (2) (pink line on the graph) exhibits “jumps” on the deformation-time dependency graph, which is a consequence of damaging the fiber during the unsatisfactory adhesive process.

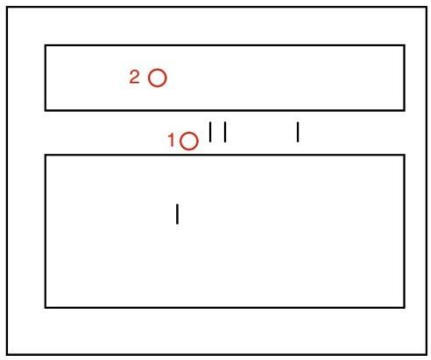

Fig. 9. Locations of the hammer impacts

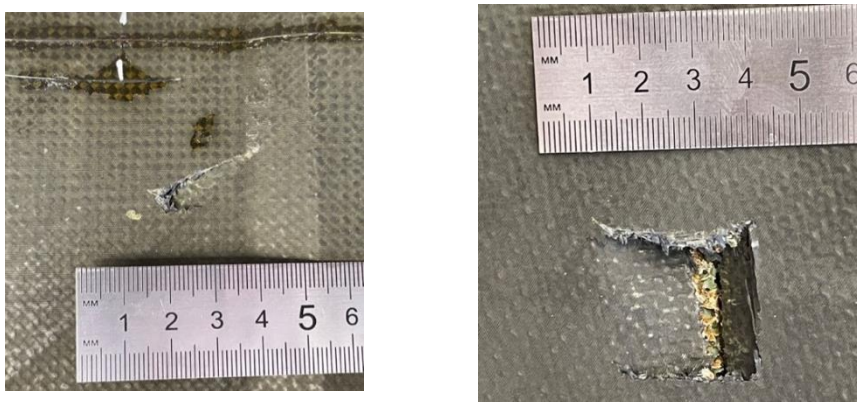

(a) (b)

Fig. 10. Appearance of the subsequent defects on the monolithic part of the panel (a) strike 1 on the monolithic part, (b) strike 2 on the honeycomb part

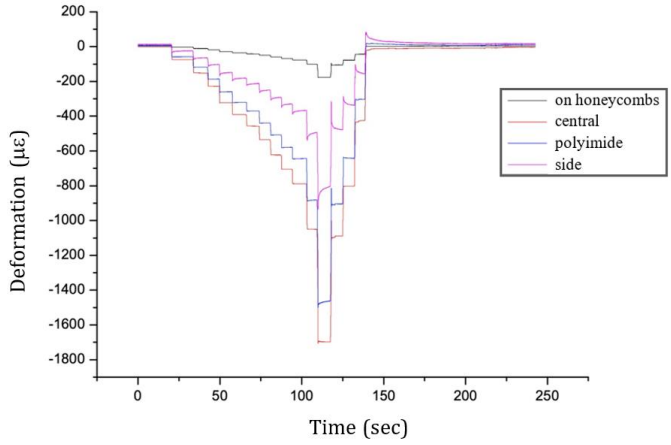

Fig. 11. The deformation-time graph resulting from static tests post-impact and post-drilling measured by three acrylic sensors and one polyimide sensor

The following description was obtained based on the comparison of static tests of each sensor before and after dynamic tests:

- acrylate sensor in the centre – Fig. 13;
- acrylate sensor on the side – Fig. 14;
- acrylate sensor on the honeycomb part – Fig. 15;
- polyimide sensor on the monolithic part – Fig. 16.

This sensor experiences the most deformations after the dynamic impacts thus proving the presence of residual stresses in the monolithic part of the panel.

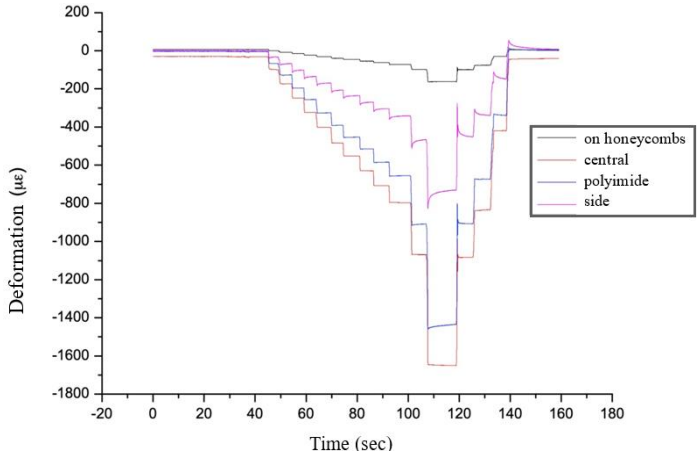

Fig. 12. The deformation-time graph resulting from static tests after fracture by hammer measured by three acrylic sensors and one polyimide sensor

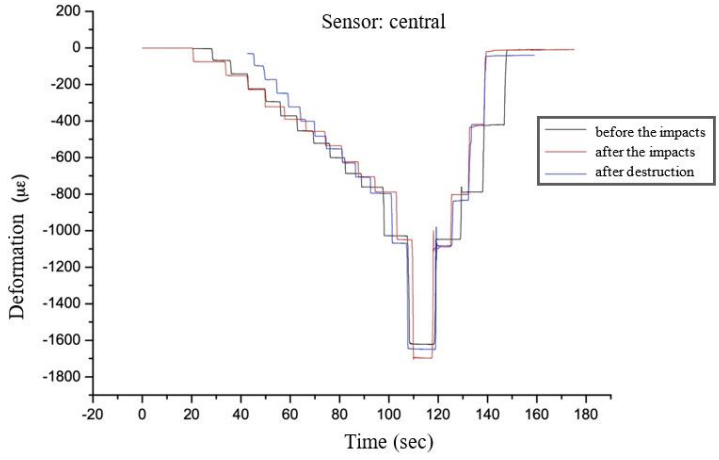

Fig. 13. The deformation-time graph resulting from three static tests measure by a single acrylate sensor (1)

The resulting data from acrylate sensor on the side (2) demonstrates uneven response (in comparison with the other sensors 1, 3 and 4) which is a consequence of a defect emerging because of a poor adhesion of the optical fiber to the panel.

The sensors used on the honeycomb part demonstrates a non-typical behaviour (in comparison with sensors 1 and 4) in the sense of the minimal deformations appearing after the destruction, rather than before any of the impacts took place. The reason for such an anomaly is not obvious and should be researched further.

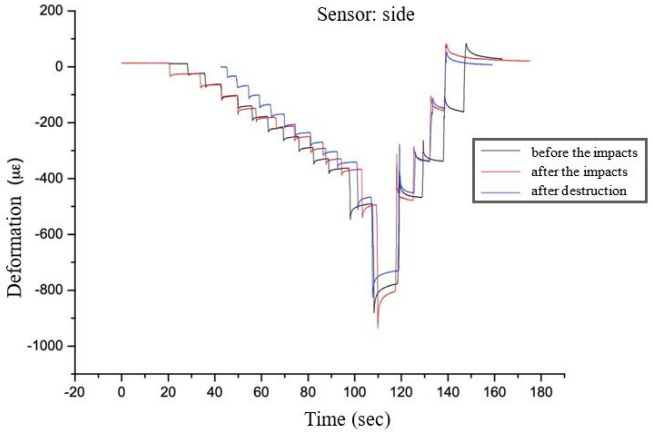

Fig. 14. The deformation-time graph resulting from three static tests measure by a single acrylate sensor (2)

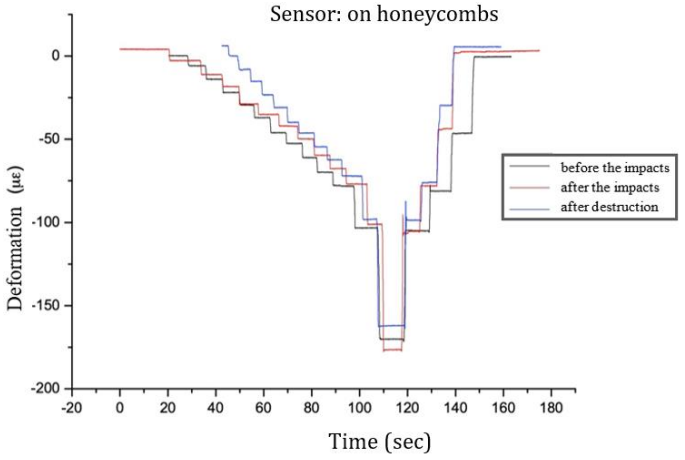

Fig. 15. The deformation-time graph resulting from three static tests measure by a single acrylate sensor (3)

It should be denoted that after each successive dynamic test the deformations of the panel increase during the static tests upon application of the similar mass. This phenomenon is relevant to detecting delamination [23]. Summing up the interim results of the studies, the following theses can be formulated:

- Fiber Bragg Grating (FBG) sensors reliably detect deformations resulting from static loads. They also have the capability to sense impact loads with clear increases in deformations, which suggests their versatility and adaptability to different types of load conditions.
- The testing results reveal an increase in deformations of the composite panel due to the stress-strain state post impacts and fracture. This indicates the sensors'

ability to monitor and reveal damage progression and structural integrity loss over time, addressing the durability of a structure.

- FBG sensors can be attached to any composite structure using cyanoacrylate adhesive but embedding the sensors is more desirable due to reduced risks of spontaneous damage.

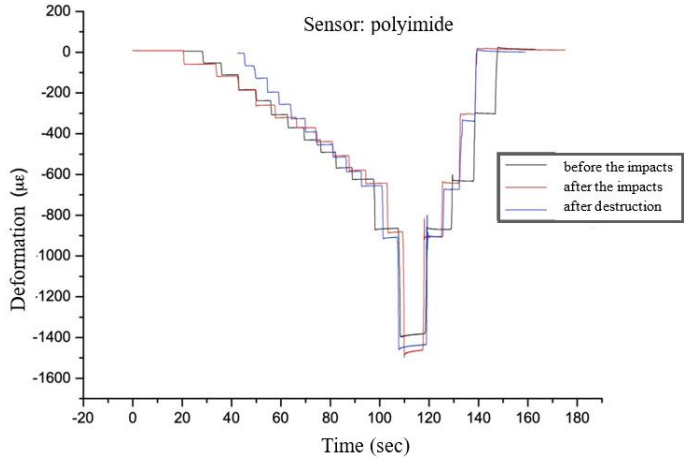

Fig. 16 – The deformation-time graph resulting from three static tests measure by a single polyimide sensor (4)

4. Conclusions

Based on the conducted study, we can conclude the following:

- Analysing the literature reveals that Fiber Bragg Grating sensors possess several distinct advantages over Rayleigh-based sensors. FBG sensors demonstrate insensitivity to variations in the quality of optical fibers, which provides a considerable degree of reliability under diverse operating conditions. This characteristic ensures their performance remains consistent even in less-than-ideal environments, thereby enhancing the robustness of the structural health monitoring systems in which they are employed.
- The stability of FBG sensor readings during the detection of deformations in static tests further corroborates their reliability. This stability is crucial for SHM applications, as it ensures that the sensors provide accurate and consistent data over extended periods, thus facilitating long-term monitoring and assessment of structural integrity.
- The equipment and software required for researching with FBG-based sensors are notably simpler and more intuitive compared to those needed for other sensor types. This simplicity allows for real-time observation and analysis of results, which significantly enhances the efficiency of data management and decision-making processes. The ease of use associated with FBG technology also reduces the training burden on personnel and minimises the likelihood of operational errors.

In summary, FBG sensing technology has demonstrated significant potential in the realm of structural health monitoring. The inherent advantages of FBG sensors, including their high sensitivity, reliability, and operational simplicity, make them a promising candidate for further study and implementation. Future research should concentrate on enhancing the reliability of FBG sensors, developing more effective data interpretation algorithms, and exploring the potential for integration with other sensor technologies. Additionally,

investigating the economic feasibility of large-scale implementation of FBG-based SHM systems in aviation is imperative. This evaluation should not only consider the direct costs associated with sensor installation and maintenance but also account for potential savings from improved maintenance efficiency, reduced downtime, and enhanced safety. By addressing these areas, future studies can pave the way for more widespread adoption of FBG technology in SHM applications, ultimately contributing to the advancement of safety and efficiency in the aviation industry.

As per detecting the exact position of an in-flight impact, a net-like structure of sensors should be installed (as one usually used in SHM systems with Rayleigh-based sensors). Further work should focus on optimising the sensor network configuration for maximum coverage and accuracy, as well as developing advanced algorithms for real-time impact detection and analysis.

Acknowledgement

The authors acknowledge that Laboratory № 3 "Modelling of composite structures" of the Center for Aerospace Materials and Technologies of the Institute № 14 "Advanced Engineering School" and Center of Composite Structures support this study in the Moscow Aviation Institute (MAI).

References

[1] Pogosyan M, Nazarov E, Bolshikh A, et al. Aircraft composite structures integrated approach: a review. J Phys Conf Ser. 2021;1925(1):21-34. https://doi.org/10.1088/1742-6596/1925/1/012005

[2] Gupta N, Augustin MJ, Sathya S, et al. Structural Health Monitoring of Composite Aircraft Structures Using Fiber Bragg Grating Sensors. J Indian Inst Sci. 2013;93(4).

[3] Sundaram R, Kamath GM, Gupta N. Structural Health Monitoring of Composite Structures-Issues and Challenges. Int J Veh Struct Syst. 2012;4(3):74-85. https://doi.org/10.4273/ijvss.4.3.01

[4] Roach D. Real time crack detection using mountable comparative vacuum monitoring sensors. Smart Struct Syst. 2009;5(4):317-328. https://doi.org/10.12989/sss.2009.5.4.317

[5] Galea SC, Velden S, Powlesland I, et al. Flight demonstrator of a self-powered SHM system on a composite bonded patch attached to an F/A-18 aileron hinge. Asia-Pacific Workshop on Structural Health Monitoring; 2006; Yokohama, Japan. p. 146-154.

[6] Arms SW, Townsend CP, Galbreath JH, et al. Flight Testing of Wireless sensing Networks for Rotorcraft Structural Health and Usage Management Systems. In: Proceedings of the Fourteenth Australian International Aerospace Congress, 7th DSTO International Conference on Health & Usage Monitoring (HUMS 2011); 2011. Corpus ID: 51946739.

[7] Friebele EJ, Askins CG, Bosse AB, et al. Optical fiber sensors for spacecraft applications. Proc SPIE. 1999;5554:120-131. https://doi.org/10.1117/12.562393

[8] McKenzie N, Karafolas N. Fiber Optic Sensing in Space Structures: The Experience of the European Space Agency. Proc SPIE. 2005;5855:262-269. https://doi.org/10.1117/12.623988

[9] Seryeznov AN, Kuznetsov AB, Lukyanov AV, et al. Application of fiber optic technologies in the creation of embedded self-diagnostic systems for aviation structures. Aviatsiya, Raketnaya i Kosmicheskaya Tekhnologiya, Nauchnyi Vestnik NSTU. 2016;64(3):95-105. doi: 10.17212/1814-1196-2016-3-95-105. https://doi.org/10.17212/1814-1196-2016-3-95-105

[10] Güemes A, Fernández-López A, Díaz-Maroto PF, et al. Structural Health Monitoring in Composite Structures by Fiber-Optic Sensors. Sensors (Basel). 2018;18(4):1094. https://doi.org/10.3390/s18041094

[11] Kosheleva NA, Shipunov GS, Voronkov AA, et al. Determination of the stress-strain state fields of samples from a polymeric composite material using fiber optic sensors. PNRPU Bull. Aerosp Technol. 2017;12(50):295-305.
[12] Shramko K, Kononov N, Ibrishev K, et al. Simulation of Adhesive Bonding of a Fiber-Optic Rayleigh Sensor with Composite Material as Part of the Design of a Monitoring System. E3S Web Conf. 2023;446:302-314. https://doi.org/10.1051/e3sconf/202344603002
[13] Качура СМ, Постнов ВИ. Перспективные оптоволоконные датчики и их применение (обзор) (Perspective optical fiber sensors and their application (review)). Trudy VIAM. 2019;5(77):52-61. https://doi.org/10.18577/2307-6046-2019-0-5-52-61
[14] Syzrantsev VN, Syzrantseva KV. Определение напряжений и остаточного ресурса по показаниям датчика деформаций интегрального типа переменной чувствительности (Determination of stresses and residual life in accordance with indications of variable sensitivity integral strain gauge). Bull Tomsk Polytech Univ Geo Assets Eng. 2017;328(9):82-93.
[15] Шершак ПВ, Яковлев НО, Орешко ЕИ. Application of optical deformation sensors for estimating the deformativity of CFRP samples near the stress concentrators. Trudy VIAM. 2022;107:111-122. https://doi.org/10.18577/2307-6046-2022-0-1-111-122
[16] Леонович ГИ, Олешкевич СВ. Гибридные датчики на волоконно-оптических брэгговских решетках (Hybrid sensors on fiber-optic bragg gratings). Izv Samar Nauch Cent Ross Akad Nauk. 2016;18(7):1340-1345.
[17] Ramlya R, Kuntjoro W, Rahman MK. Using Embedded Fiber Bragg Grating (FBG) Sensors in Smart Aircraft Structure Materials. Procedia Eng. 2012;41:600-606. https://doi.org/10.1016/j.proeng.2012.07.218
[18] Kister G, Winter D, Badcock RA, et al. Structural health monitoring of a composite bridge using Bragg grating sensors. Part 1: Evaluation of adhesives and protection systems for the optical sensors. Compos Struct. 2007;29(3):440-448. https://doi.org/10.1016/j.engstruct.2006.05.012
[19] Ye Q, Quan-bao W, Hai-tao Z, et al. Review on Composite Structural Health Monitoring Based on Fiber Bragg Grating Sensing Principle. J Shanghai Jiaotong Univ (Sci). 2013;18(2):129-139. https://doi.org/10.1007/s12204-013-1375-4
[20] Trutzel MN, Wauer K, Betz D, et al. Smart sensing of aviation structures with fiber optic Bragg grating sensors. In: Proceedings of the Smart Structures and Materials 2000: Sensory Phenomena and Measurement Instrumentation for Smart Structures and Materials; 2000. p. 134-143. https://doi.org/10.1117/12.388099
[21] Zhou Y, Zhao Y, Liu D, et al. Review on Structural Health Monitoring in Metal Aviation Based on Fiber Bragg Grating Sensing Technology. In: Proceedings of the 2020 Prognostics and Health Management Conference (PHM-Besancon); 2020. p. 97-102. https://doi.org/10.1109/PHM-Besancon49106.2020.00022
[22] Dong T, Kim NH. Cost-Effectiveness of Structural Health Monitoring in Fuselage Maintenance of the Civil Aviation Industry. Aerospace. 2018;5(4):87. https://doi.org/10.3390/aerospace5030087
[23] Tinchurina D, Kononov N, Permyakov A, et al. Registration of the Growth of Manufacturing Defects by the Monitoring System During the Operation of the Structure. E3S Web Conf. 2023;446:34-43. https://doi.org/10.1051/e3sconf/202344603003